

# Parameters affecting the flexural capacities of reinforced concrete members strengthened with FRP strip: A critical comparison

A. Hasnat

*University of Asia Pacific, Dhaka, Bangladesh*

M.M. Islam

*Ahsanullah University of Science and Technology, Dhaka, Bangladesh*

A.F.M.S. Amin

*Bangladesh University of Engineering and Technology, Dhaka, Bangladesh*

**ABSTRACT:** Fiber reinforced polymer (FRP) strengthened flexural members fail primarily due to rupture of FRP and crushing of concrete, after or before yielding of steel. The secondary mode of failure is related to the debonding or delamination of the FRP strips. However, available codes and literatures do not provide clear basis on the ascertaining factors that affect the failure modes. To this end, it becomes difficult to predict the actual failure mode and consequently the enhancement of the moment capacity after strengthening as well. In this paper, factors influencing the enhancement of the moment capacities of FRP strengthened flexural members considering the primary modes of failure are analyzed with respect to available codes and literatures. Compressive strength of concrete, substrate strains, modulus of elasticity and tensile strength of FRP, effective depth of concrete, width of FRP strip are logically varied to understand respective contributions in the enhancement of moment capacity.

## 1 INTRODUCTION

The moment capacity of structural members strengthened for flexure depends on the mode of failure. The failure of FRP strengthened flexural members may occur due the rupture of FRP and crushing of concrete, after or before yielding of steel. The primary failure modes are therefore defined as, Mode 1a: Concrete crushing after steel yields, Mode 1b: Concrete crushing before steel yields, Mode 2a: FRP failure after steel yields, Mode 2b: FRP failure before steel yields (Bank 2006, Fig 1). To arrive at a solution, one of the four failure modes above must first be assumed. Thereafter, the location of the neutral axis,  $c$ , for this assumed failure mode is determined either by a trial-and-error method (ACI 2008) or by solving a quadratic equation (Bank 2006). The correct value of  $c$  is the unique solution that gives the stresses and strains in the materials that are compatible with the assumed failure mode. It is important to point out that in most practical strengthening designs it is generally accepted that the failures should be in mode 1a or mode 2a; that is, failure occurs in the concrete or the FRP after the internal tension steel has yielded. This is because most FRP strengthening systems have lower moduli and higher strains to failure than the internal reinforcing steel bars, and they are located a similar distance from the neutral axis of the section (i.e.,  $d$  or  $h$ ). To utilize the large strain capacity of FRP strengthening systems effectively, the strain in the steel at failure of the strengthened system needs to be much larger than the yield strain of steel, which is 0.00207 for grade 60 rebar. However, for very high modulus strengthening systems, that have lower strains to failure, such as ultrahigh-modulus carbon systems, substantial strengthening can be achieved without the steel yielding before failure (Modes 1b and 2b). In addition, for specific geometries and FRP strengthening configurations it may not be possible to achieve steel yielding before failure (because of FRP detachment, or an existing high reinforcement ratio, or a very low strength concrete). Also, in some designs the driving design requirement, generally when excessive live loads are a concern, is to reduce the strain in the internal steel at service loads. In these cases, failure after steel yielding is not a desirable failure mode.

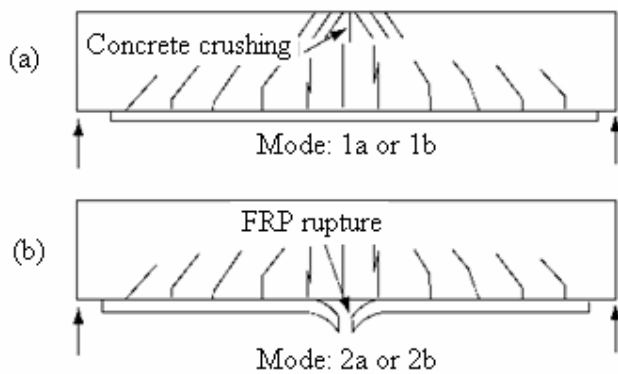


Figure 1. Primary failure modes (a) Mode: 1a or 1b, (b) Mode: 2a or 2b.

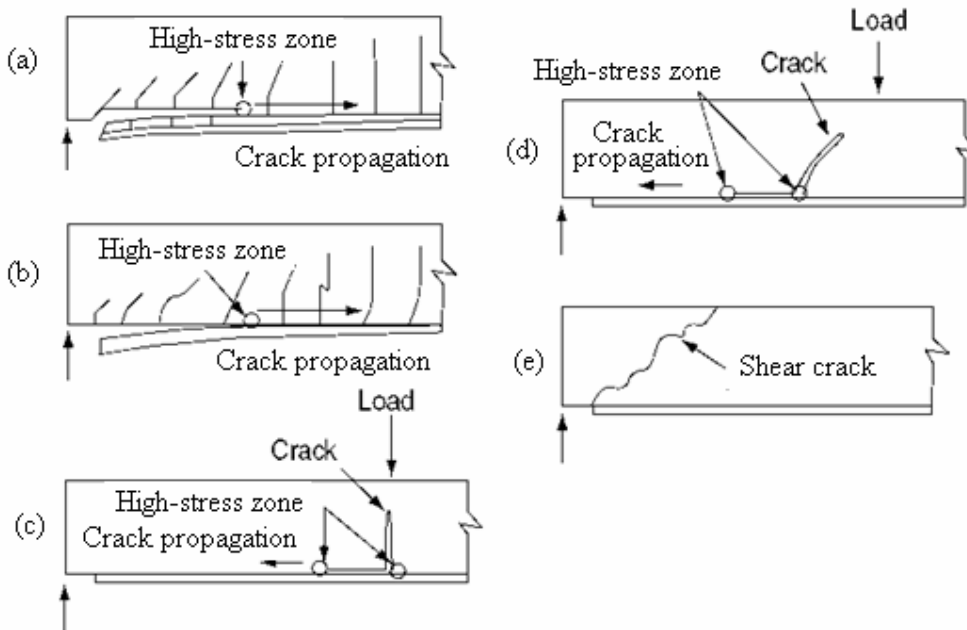


Figure 2. Debonding failure modes, (a), (b), (c), (d) types of debonding failure, (e) shear failure.

## 2 PROTOTYPE STRUCTURE

The analysis is done based on evaluating the analytical formulas given by Bank (2006) and ACI (2008) with the experimental results of recently tested FRP strengthened flexural members prototype structures. The cross sections of the flexural members are considered 280 mm (11 in) depth and 650 mm (25.6 in) width with 3.6 m (11.81 ft) span length (Fig 3). The loading is applied in both unstrengthened and strengthened specimens to observe the moment capacity enhancement due to FRP system and also the governing failure modes. In the experiment, the width of the FRP is 150 mm (6 in) and the thickness is 1.4 mm (0.055 in). The concrete compressive strength is 48 MPa (7000 psi) and the yield strength of the steel was 414 MPa (60000 psi). The tensile strength FRP is 2390 MPa and elastic modulus 157.57 GPa. The tests are done in room temperature and also in high temperature. The compressive strength of concrete, substrate strains, modulus of elasticity and tensile strength of FRP, effective depth of concrete, width of FRP strip are logically varied using formulae and failure modes given by Bank (2006) and ACI (2008). Table 1 presents the parameters and the variation range.

## 3 ANALYTICAL METHODS

### 3.1 ACI 440.2R-08. (2008)

According to ACI (2008), initially the depth of neutral axis ( $c$ ) is assumed  $0.2d$  and then it is evaluated using the Equation 1. The value of  $c$  is fixed by trial and error.

Table 1. The variation range of controlling parameters

Parameters	Unit	Range of variation
Compressive strength of concrete, $f'_c$	psi	3000, 4000, 5000, 6000, 7000, 8000
Modulus of elasticity of FRP, $E_f$	ksi	6000, 10000, 20000, 25000
Tensile strength of FRP, $f_{fe}$	ksi	100, 200, 300, 400
Effective depth of concrete, $d$	in	9, 10, 10.5
Width of FRP strip, $w_f$	in	2, 4, 8, 12, 16, 20, 24

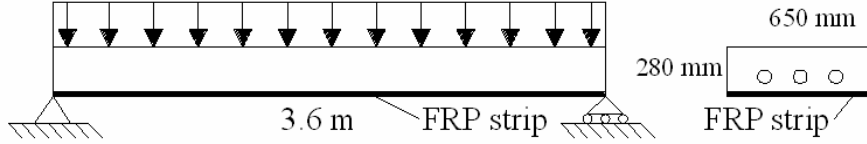


Figure 3. The prototype structural member.

$$c = \frac{A_s f_s + A_f f_{fe}}{\alpha_1 f'_c \beta_1 b} \quad (1)$$

where  $\alpha_1$  and  $\beta_1$  are approximate stress block factors,  $A_s$ = area of steel,  $A_f$ = area of FRP,  $f_s$ =stress in steel,  $f_{fe}$ = stress in FRP,  $f'_c$  = compressive strength of concrete and  $b$  = width of the member. FRP contribution in moment capacity enhancement is calculated as Equation 2.

$$M_{nf} = A_f f_{fe} \left( d_f - \frac{\beta_1 c}{2} \right) \quad (2)$$

where  $d_f$ = depth of FRP strip from the compression face.

### 3.2 Bank (2006)

#### 3.2.1 Mode 1a: concrete crushing after steel yields

According to Bank (2006) and considering the failure Mode: 1a, the depth of the neutral axis is calculated solving the quadratic equation of Equation 3.

$$(0.85 f'_c \beta_1 b) c^2 - A_s f_y c - A_f E_f [\varepsilon_{cu} (h - c) - \varepsilon_{bi} c] = 0 \quad (3)$$

where  $E_f$  = modulus of elasticity of FRP,  $\varepsilon_{cu}$  = ultimate strain of concrete,  $f_y$  = yield stress of steel and  $h$  = depth of the flexural member. The contribution of FRP in moment capacity enhancement is calculated using Equation 4.

$$M_n = \psi_f A_f f_{fe} \left( h - \frac{\beta_1 c}{2} \right) \quad (4)$$

#### 3.2.2 Mode 1b: concrete crushing before steel yields

According to Bank (2006) and considering the failure Mode: 1b, the depth of the neutral axis is calculated solving the quadratic equation of Equation 5.

$$(0.85 f'_c \beta_1 b) c^2 - A_s E_s \varepsilon_{cu} (d - c) - A_f E_f [\varepsilon_{cu} (h - c) - \varepsilon_{bi} c] = 0 \quad (5)$$

The FRP contribution is calculated using Equation 4.

### 3.2.3 Mode 2a: FRP failure after steel yields

According to Bank (2006) and considering the failure Mode: 2a, the depth of the neutral axis is calculated solving the quadratic equation of Equation 6.

$$c = \frac{A_s f_y + A_f \kappa_m f_{fu}}{0.85 f'_c \beta_1 b} \quad (6)$$

where  $A_s$ = area of steel,  $\kappa_m$ = bond-dependent coefficient and  $f_{fu}$ = ultimate tensile strength of FRP. The FRP contribution is calculated using Equation 4.

### 3.2.4 Mode 2b: FRP failure before steel yields

According to Bank (2006) and considering the failure Mode: 2a, the depth of the neutral axis is calculated solving the quadratic equation in Equation 7.

$$(0.85 f'_c \beta_1 b) c (h - c) - A_s E_s (\varepsilon_{fe} + \varepsilon_{bi}) (d - c) - A_f E_f \varepsilon_{fe} (h - c) = 0 \quad (7)$$

The FRP contribution is calculated using Equation 4.

## 4 MOMENT CAPACITY IN PRIMARY FAILURE

### 4.1 Mode 1a, 2a (low steel ratio)

According to Bank (2006) and ACI (2008), the design parameters are varied and analyzed for the enhancement of the moment capacity. With low steel area (reinforcement), the Mode 1a and 2a are likely to occur. The percentage increase of moment capacity is found linear with increase of modulus of elasticity of FRP according to ACI (2008) in Figure 4. But for Bank (2006), it is found nonlinear for both Mode 1a and 2a (Fig 4).

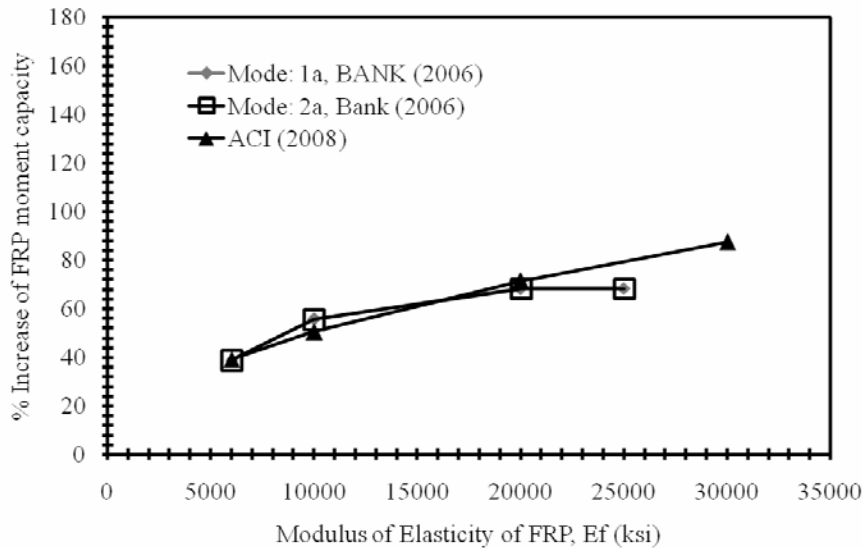


Figure 4: Enhancement of the moment capacity due to FRP with increasing Modulus of elasticity of FRP

The effective depth of the concrete is found to be another governing parameter controlling the failure as well as the enhancement of the moment capacity using FRP system. High effective depth of concrete provides low concrete cover and raise the possibility of debonding of concrete due to spalling. It is also clear from the Figure 5. The reduction of moment capacity occurs with the increase of effective depth for both the modes 1a and 2a for Bank (2006) and ACI (2008).

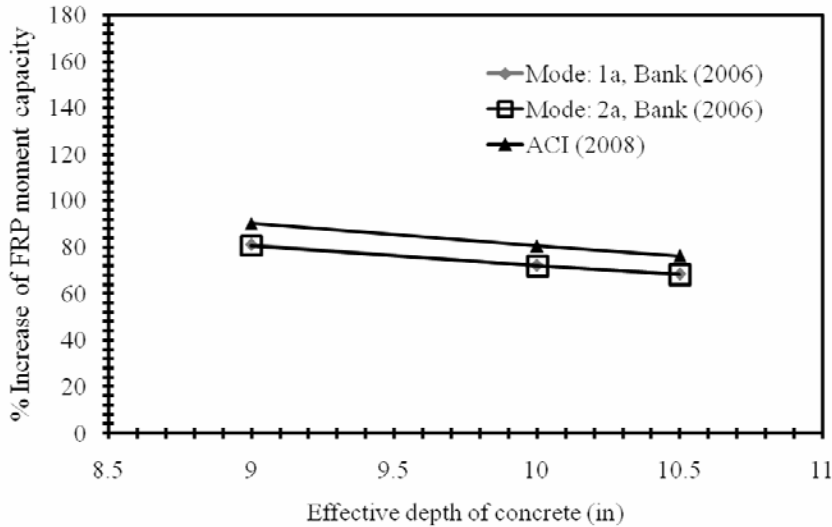


Figure 5: Reduction of the moment capacity due to FRP with increasing effective depth of concrete.

The percentage increase of the moment capacity is found to be increased proportionally with compressive strength of concrete for ACI (2008). But for Bank (2006), the increment is found nonlinear for both the cases of failure (Figure 6).

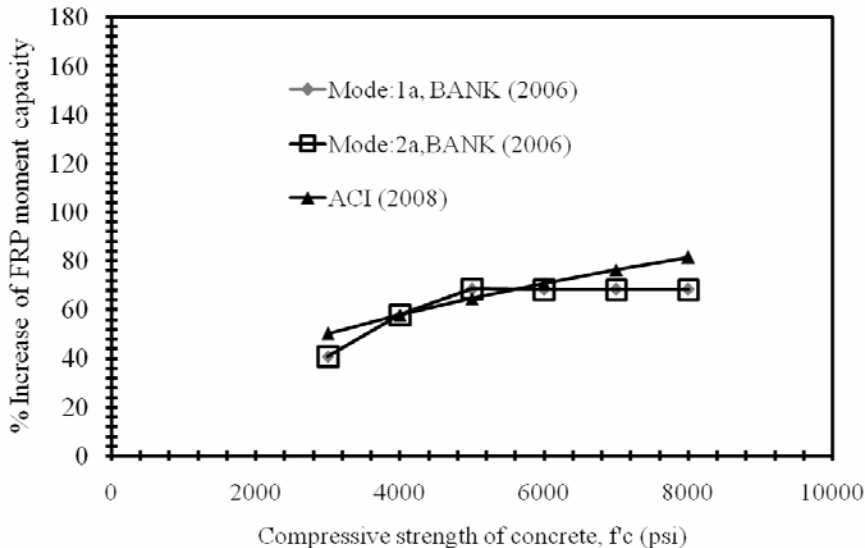


Figure 6: Enhancement of the moment capacity due to FRP with increasing compressive strength of concrete.

The enhancement of moment capacity is found to be linearly varied with the width of FRP strips as per ACI (2008) and Bank (2006) in Figure 7.

#### 4.2 Mode 1b, 2b (high steel ratio)

With high steel ratio and failure modes 1b or 2b, the enhancement of moment capacity is insignificant (Figure 8 and 9). Contribution of FRP is less, if the provided steel reinforcement of high (Figure 10).

### 5 MOMENT CAPACITIES IN DELAMINATION FAILURE

#### 5.1 Current method (considering $\kappa_m$ )

The analytical methods to predict the various detachment (also known as delamination or debonding) failure modes are still not fully developed, and the ACI (2002 and 2008) guide does not provide an explicit procedure to determine whether or not a detachment failure will occur. Instead, the ACI guide limits the strain permitted in the FRP strengthening system to ensure that none of the detachment failure modes [(a) to (e)] in Fig-

ure 2] is likely to occur. The maximum effective tensile strain in the FRP strengthening system,  $\epsilon_{fe}$ , is obtained by multiplying the design ultimate rupture strain,  $\epsilon_{fu}$ , by an empirically obtained bond-dependent coefficient,  $\kappa_m$ , which is a function of the stiffness and thickness of the FRP system and defined as Equation 8 (ACI 2002):

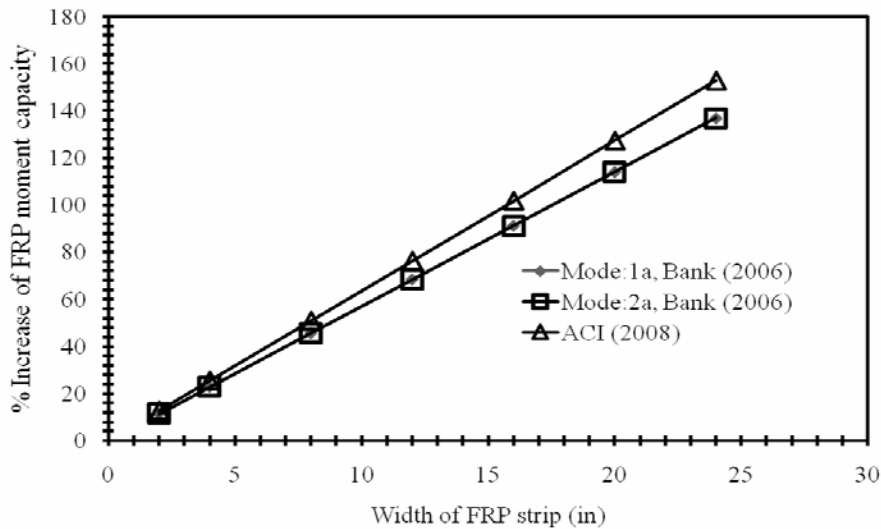


Figure 7: Enhancement of the moment capacity due to FRP with increasing FRP strip width.

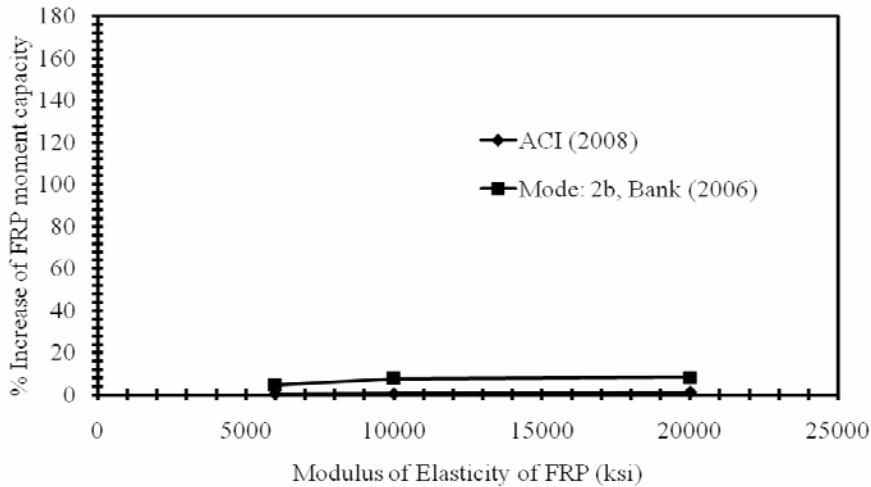


Figure 8. Enhancement of the moment capacity due to FRP with increasing modulus of elasticity of FRP (considering steel are 20in<sup>2</sup>).

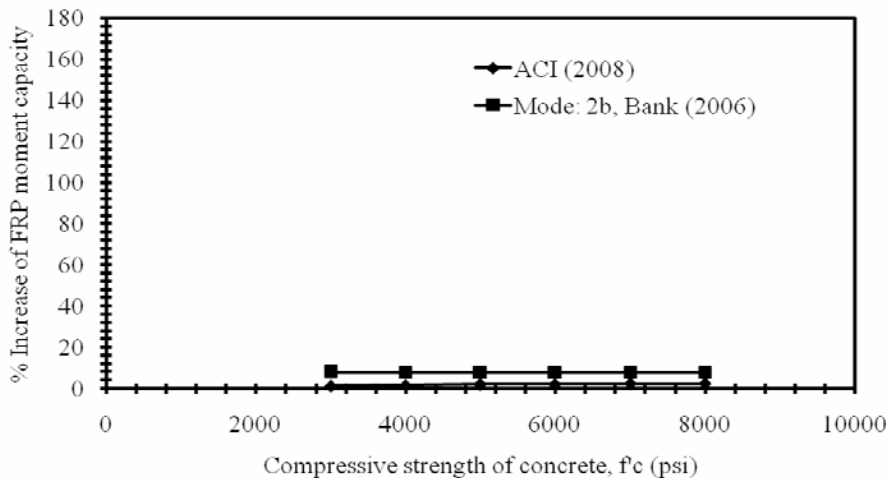


Figure 9. Enhancement of the moment capacity due to FRP with increasing compressive strength of concrete (considering steel are 20in<sup>2</sup>).

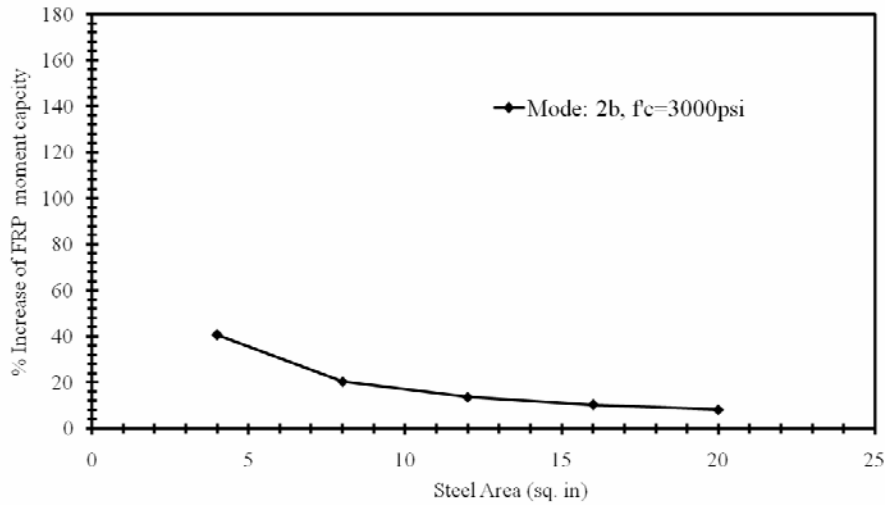


Figure 10. Effect of steel area with FRP moment capacity.

$$\kappa_m = \begin{cases} \frac{1}{60\varepsilon_{fu}} \left( 1 - \frac{nE_f t_f}{2,000,000} \right) \leq 0.90, \text{ for } nE_f t_f \leq 1000000 \text{ lb/in} \\ \frac{1}{60\varepsilon_{fu}} \left( \frac{500,000}{nE_f t_f} \right) \leq 0.90, \text{ for } nE_f t_f > 1000000 \text{ lb/in} \end{cases} \quad (8)$$

where  $n$  is the number of layers (or plies) of FRP strips or sheets or fabrics,  $E_f$  the longitudinal tensile modulus of the FRP composite in the case of strips or the longitudinal modulus of the fibers in the strengthening direction in the case of sheets or fabrics, and  $t_f$  the thickness of an individual strip in the case of FRP strips or the net thickness of the fibers in a single sheet or fabric in the case of sheets or fabrics. Since  $\kappa_m$  must be less than 0.9, the strain in the FRP is never allowed to reach the ultimate rupture strain in the ACI design procedure. Therefore, theoretically, the failure mode of FRP rupture [(a) in Figure 1] can never occur, according to the ACI. According to the ACI 440.2R-02 guide, only two failure modes are assumed to occur for the purposes of design calculations: compressive failure of the concrete (mode 1a) and failure of the FRP strengthening system (mode 2a). For each of these design failure modes, the stress in the FRP, the internal steel, and the concrete are required to determine the ultimate bending capacity of the section.

### 5.2 Effect of $f'_c$

The FRP system is attached to the tension face of the concrete. It is conditional that, the debonding or delaminating of FRP is to depend on the properties of concrete e.g. compressive strength or tensile strength. The formula of the bond-dependent coefficient,  $\kappa_m$ , given in Equation 1, shows no trace of dependency on the compressive strength ( $f'_c$ ). The value of  $\kappa_m$  is found not reliable to predict the possibility of debonding or delamination failure of FRP system from the concrete surface and must be revised by adequate experimental tests.

### 5.3 Existing substrate strain

Since the FRP strengthening system is attached to the existing deflected structure, strains will already exist in the steel and concrete prior to the FRP being attached. These existing strains must be accounted for in the design process if the member is not shored up during the strengthening operation. Neglecting the existing strain in the concrete will lead to unconservative designs. To illustrate the strain conditions in the strengthened beam, the strains in the section can be depicted as a superposition of strains from before and after the FRP is attached, as shown in Figure 3. The three strain states depicted are (1) the initial state: before the FRP is attached, considering only the existing load at the time the FRP is attached; (2) the strengthened state: after the FRP has been attached, considering only the supplemental loads that are applied after the FRP has been attached (a hypothetical situation); and (3) the final state: after the FRP has been attached with the existing and

supplemental loads. Notice how the strain in the initial state is added to the strain that develops in the FRP strengthening system to give the final strain state at the underside of the beam. This final strain at the underside of the beam must be compatible with the strain in the concrete in the final state. It is noticeable, how the neutral axis shifts position in the three states.

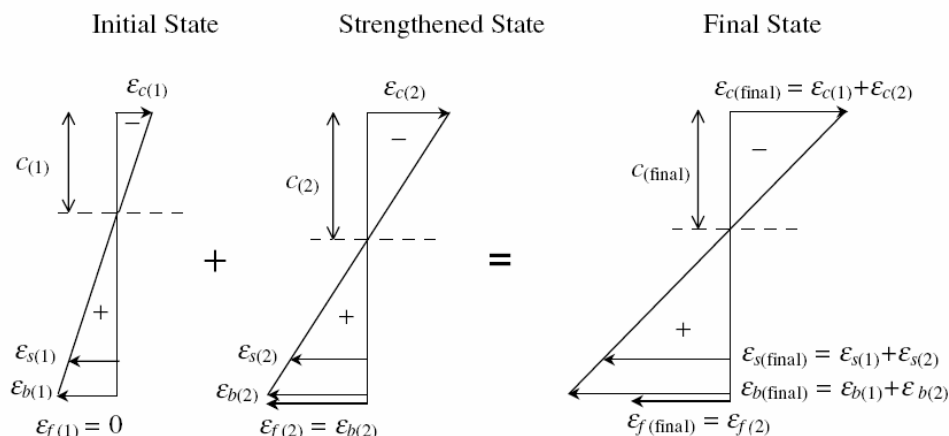


Figure 3. Superposition of strain after strengthening.

In ACI 440.2R-02 the existing strain at the substrate,  $\varepsilon_{b(1)}$ , is identified as  $\varepsilon_{bi}$  and can be found from the properties of the transformed cracked section using Equation 9.

$$\varepsilon_{bi} = \frac{m_l(h - k_1d)}{(I_{cr})_1 E_c} \quad (9)$$

where  $m_l$  is the service load moment in the beam at the time the FRP system is attached (typically, only the dead load on the beam). The remaining terms are the usual properties of the transformed cracked section of the unstrengthened beam.

## 6 CONCLUSIONS

The design parameters are critically analyzed according to Bank (2006) and ACI (2008) considering available failure modes. Though, there exists no trace of concrete compressive or tensile strength in determining bond-coefficient ( $\kappa_m$ ), in most of the cases with varying parameters, the governing failure modes are Mode: 1a and 2a. No significant difference was found the obtained moment capacity using formulae of Bank (2006) and ACI (2008) with respect to width of FRP strip. The reduction of moment capacity enhancement is found due to increase of concrete effective depth as the possibility of debonding arises. The enhancement of moment capacity is existing compressive strength of concrete and the modulus of elasticity of FRP. The variation is linear for ACI (2008) but for Bank (2006), it varies nonlinearly. The formula of  $\kappa_m$  is recommended to revise with the significance of concrete strength to predict the debonding or delamination of FRP strips.

## REFERENCES

- ACI 440.2R-02. 2002. Guide for the Design and Construction of Externally Bonded FRP Systems for Strengthening Concrete Structures, American Concrete Institute, Reported by ACI Committee 440.
- ACI 440.2R-08. 2008. Guide for the Design and Construction of Externally Bonded FRP Systems for Strengthening Concrete Structures. American Concrete Institute, Farmington Hills, MI.
- Bank, L.C. 2006. Composites for Construction: Structural Design with FRP Materials. New Jersey: John Wiley & Sons, Inc.